AD-A093 488 CORNELL UNIV ITHACA N Y DEPT OF AEROSPACE ENGINEERING F/G 20/4
A LEAST SQUARE FINITE ELEMENT TECHNIQUE FOR TRANSONIC FLOW WITH--ETC(U)
AUG 77 A R WADIA N00014-75-C-0375
UNCLASSIFIED NL

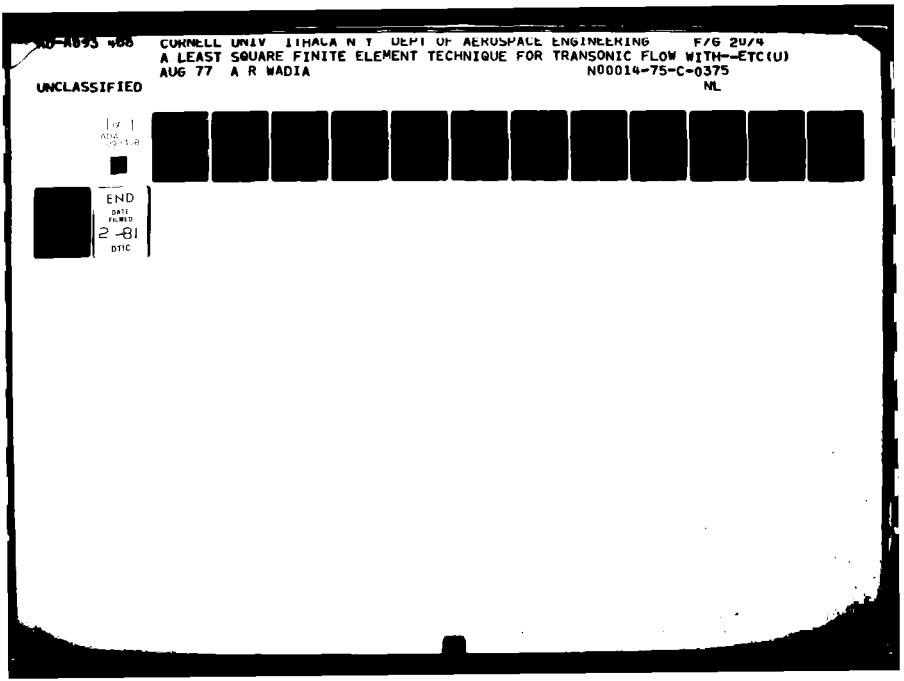

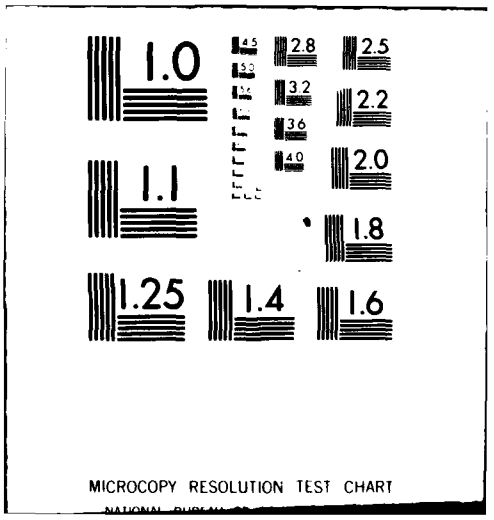
1.0
1.1
1.25
1.4
1.6
1.8
2.0
2.2
2.5
2.8
3.2
3.6
4.0
MICROCOPY RESOLUTION TEST CHART

A LEAST SQUARE FINITE ELEMENT TECHNIQUE FOR TRANSONIC FLOW [illegible]

Aspi Rustom Wadia
Cornell University
Ithaca, New York

(15) N00014-75-C-0375
AFOSR-74-2659
(10) 09855
(11) 22 AUG 77

Abstract

The governing differential equation for the one-dimensional, transonic flow in a laval nozzle in the vicinity of the throat was obtained in the non-dimensional form. A least square finite element technique was used with a linearly interpolating polynomial to reduce the governing equation to a system of non-linear algebraic equations which were solved numerically by Newton's method. The system of partial differential equations for the two dimensional flow in a laval nozzle was also obtained in the non-dimensional form. The method of integral relations was used to replace the original system of partial differential equations by a system of ordinary differential equations. Using the least square finite element technique a computer program was developed for the construction and solution of the non-linear equations for the laval nozzle problem. The results including the location of the shock in the flow are presented.

I. Introduction

No other aspect of transonic flow has been the subject of serious study for nearly so long as that of flows in ducts and nozzles. It is remarkable that the essential features of steady accelerating one dimensional flows at speeds up to and beyond the speed of sound had been well described and understood by the end of the last century, before the rapid development of modern fluid mechanics, and a realistic analysis on a one dimensional basis proved possible. In particular, because viscous effects in continuously accelerating nozzle flows are small, the concept of boundary layer was not essential for progress.

The survey papers of Hall and Sutton[1] and of Sichel[2] outline progress with theories for nozzle flow, the latter paper in the wider context of viscous transonic flow. Other newer techniques are due to Moretti[4] adapted by Midgal[3,4] et.al. and Thompson[5]. Holt[6] and others have introduced to the nozzle problem the method of integral relations which had been successful in solving other transonic flow problems.

The problem of transonic flow in nozzles is difficult because the governing equations are of the mixed type, changing from elliptic in the low speed region near the nozzle entry to hyperbolic in the supersonic region. In two dimensional irrotational flow, the problem can be solved by the hodograph method, developed successively by Lighthill[7], Frankl[8] and Cherry[9,10,11]. In spite of its high state of development, the hodograph method has limitations. It can only be applied to the design problem in plane flow and cannot be used in the direct problem of calculating the flow field corresponding to a given contour. It does not apply at all to axially symmetric flow since the presence of the radial term in the equation of continuity destroys the linear character of the hodograph equations.

For such problems of more general character it is necessary to work in the physical plane and solve the governing system of non-linear equations as they stand. Taylor[12] used series expansion in the neighborhood of the sonic throat, Oswatitsch and Rothstein[13] developed an iterative technique and Emmons[14] calculated the flow in a hyperbolic nozzle by a relaxation method. (12) 12

A recent publication on the use of the method of integral relations for transonic flow in nozzles has been published by Liddle[15,16]. Chen[17], in his finite element solution to the nozzle problem was unable to predict the location of a shock in the flow. Liddle's[15,16] method to be valid requires that there be no shocks in the flow and though this method can give solutions extending into the supersonic region, the solutions are invalid if there are shock waves or local wall curvature discontinuities.

This paper sets out to solve the direct problem of transonic flow in a laval nozzle and to determine the location of the weak shock using a least square finite element technique.

The governing equation derived in the following section can be solved exactly by analytical methods and so it was selected as a model equation to illustrate the numerical method and also because the accuracy of the numerical computation could be compared with the exact solution, the ultimate aim being to use the numerical method developed in this paper for similar problems with shocks.

II. Assumptions and Basic Equations For One-Dimensional Flow

Consider one-dimensional, isentropic, steady, inviscid, transonic flow in a nozzle of varying cross-sectional area subject to no wall friction and heat exchange with the walls. The equations of continuity and momentum are

$$d(\rho AU) = 0 \qquad (1)$$

$$UdU + \frac{dp}{\rho} = 0 \qquad (2)$$

where, ρ is the density, A is the area of cross-section, U is the velocity and p is the pressure. For isentropic flow the speed of sound, a, is related to the compressibility of the fluid by

$$a^2 = \frac{dp}{d\rho} \qquad (3)$$

Research jointly supported by the Air Force OSR under Grant AFOSR-74-2659, and the U.S. Navy ONR Grant N00014-75-C-0375.

Graduate Research Assistant, Department of Aerospace Engineering, Cornell University. Student Member, AIAA.

DISCLAIMER NOTICE

THIS DOCUMENT IS BEST QUALITY PRACTICABLE. THE COPY FURNISHED TO DTIC CONTAINED A SIGNIFICANT NUMBER OF PAGES WHICH DO NOT REPRODUCE LEGIBLY.

Substituting Eq. (3) in

$$UdU + \frac{a^2}{\rho} d\rho = 0 \qquad (4)$$

Eq. (1) can be written as

$$UAd\rho + \rho d(UA) = 0 \qquad (5)$$

Substituting for $d\rho$ from Eq. (5) in Eq. (4) and using the relation $M = U/a$ where M is the mach number, gives on simplication

$$\frac{d(U^2)}{dx} - \frac{2U^2}{M^2-1} \frac{1}{A} \frac{dA}{dx} = 0 \qquad (6)$$

The energy equation in differential form is

$$d(a^2 + \frac{\gamma-1}{2} U^2) = 0 \qquad (7)$$

where γ is the ratio of specific heats. Differentiating each side of the relation $M^2 = (\frac{U}{a})^2$ and substituting for $d(a^2)$ from Eq. (7) gives on simplification

$$d(U^2) = \frac{a^2 d(M^2)}{1 + \frac{\gamma-1}{2} M^2} \qquad (8)$$

Substituting for $d(U^2)$ from Eq. (8) into Eq. (6) and simplifying yields

$$\frac{d(M^2)}{dx} + \frac{2(1 + \frac{\gamma-1}{2} M^2)M^2}{1 - M^2} \frac{1}{A} \frac{dA}{dx} = 0 \qquad (9)$$

Assuming transonic flow, let

$$M^2 = 1 + \delta \qquad (10)$$

where $\delta \ll 1$. Assuming a parabolic wall shape, let

$$A = 1 + \alpha x^2 \qquad (11)$$

where α is some constant depending on the nozzle geometry. Differentiating Eqs. (10) and (11) with respect to x and substituting in Eq. (9) gives

$$\frac{d\delta}{dx} + \frac{2(1 + \frac{\gamma-1}{2} M^2)M^2}{1-M^2} \frac{1}{1+\alpha x^2} 2\alpha x = 0 \qquad (12)$$

Expanding $(1+\alpha x^2)^{-1}$ in a Taylor series for small x, i.e. in the vicinity of the throat and substituting Eq. (10) in Eq. (12) and neglecting $0(x^2)$ and $0(\delta^2)$ terms, Eq. (12) reduces to

$$\frac{d(\delta^2)}{dx} - 4(\gamma+1)\alpha x(1 + \frac{2\gamma}{\gamma+1} \delta) = 0 \qquad (13)$$

Eq. (13) was scaled to give the one-dimensional equation of transonic flow in a laval nozzle in the normalized form as

$$\frac{d(V^2)}{d\xi} - \xi(1-V) = 0 \qquad (14)$$

where

$$V = -\frac{2\gamma}{\gamma+1} (M^2-1) \qquad (15)$$

and

$$\xi = 4\gamma \sqrt{\frac{\alpha}{\gamma+1}}\, x \qquad (16)$$

Finally, since this paper will be primarily concerned with discontinuous solutions, it is necessary to apply the jump condition

$$[V^2] = 0 \qquad (17)$$

which must be satisfied by weak solutions of Eq. (14).

III. Statement and Physical Concepts of the Laval Nozzle Problem

The one dimensional nozzle problem involves the solution of the non-linear ordinary differential equation, Eq. (14) with the boundary conditions at the entry and the exit being specified as

$$V(-a) = V_1, \; V(a) = V_n$$

where V_n is greater than V_1 and the jump condition is as indicated by Eq. (17).

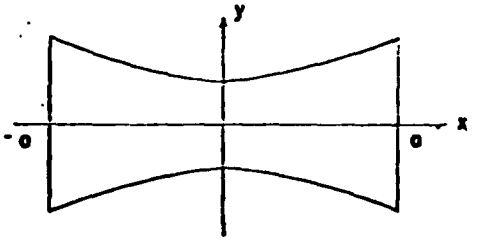

Figure 1. Laval nozzle.

Eq. (14) is a first order differential equation which has to satisfy two boundary conditions and thus it is difficult to obtain the correct solution with shock using standard numerical methods. Several numerical techniques were investigated and the least square finite element technique developed gave the desired results.

Solving Eq. (14) analytically gives

$$\frac{\xi^2}{4} + \text{constant} = \ln(\frac{1}{1-V}) - V \qquad (18)$$

For a sonic throat $V = 0$ at $\xi = 0$, thus

$$\frac{\xi^2}{4} = \ln(\frac{1}{1-V}) - V \qquad (19)$$

Eq. (15) indicates that for $M > 1$, V is negative and for $M < 1$, V is positive. Using (19), the two branches of the laval nozzle curve are sketched in figure 2. If the flow in the nozzle was from left to right four solutions are possible, depending on the value of the entry and exit Mach numbers.

Eq. (14) can have a subsonic solution in which the flow accelerates from the inlet to the throat and decelerates downstream of the throat and exits at subsonic speed (3-2, figure 2). A continuously

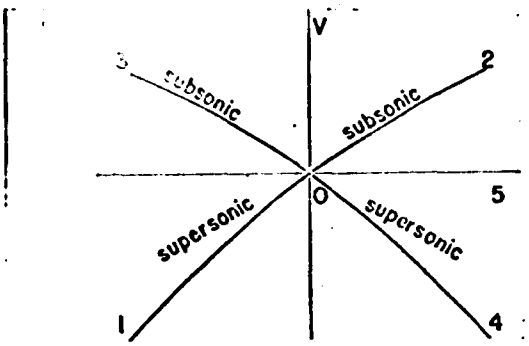

Figure 2. Two branches of the Laval nozzle curves

accelerating flow solution can also be obtained in which the flow enters with subsonic speed, attains a Mach number of unity in the throat section and exits from the nozzle at supersonic speed (3-4, figure 2). A solution that would be obtained for a supersonic diffuser in which the flow could enter with a supersonic velocity, decelerate to reach the sonic speed in the throat and exit again with subsonic speed is the curve 1-2 shown in figure 2. If $V_n > V_1$, the flow will enter with subsonic speed, become sonic in the throat, attain supersonic speed downstream of the throat, have a jump in velocity through a shock and exit with a subsonic velocity from the nozzle. The two possible solutions of interest in this paper are shown in figures 3 and 4.

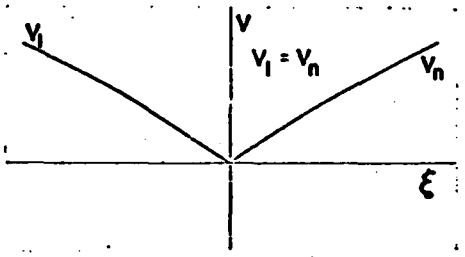

Figure 3. The subsonic solution

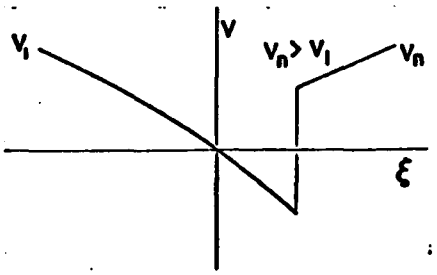

Figure 4. The solution with shock

Specifying V_n, the exit condition, the value of the constant in Eq. (18) can be determined and the shock location in the model example can be obtained graphically. Using Eq. (19) AOB was plotted as shown in figure 5. OC was then plotted as a mirror image of OB about the ξ-axis. Using V_n, the constant in Eq. (18) was determined and the curve DEHJ was plotted on the same figure. DEHJ intersects the reflected curve OC at E, thus giving the location of the discontinuity. The shock solution is represented by AOGFED with the jump condition GF = EF satisfying Eq. (17). The complete set of laval nozzle curves are plotted in figure 6.

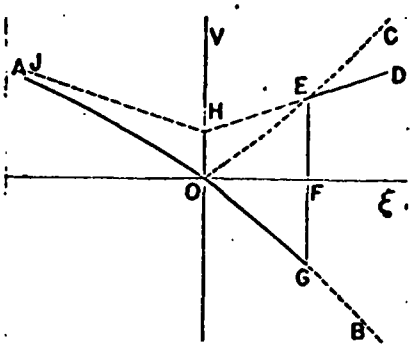

Figure 5. Graphical determination of the shock solution.

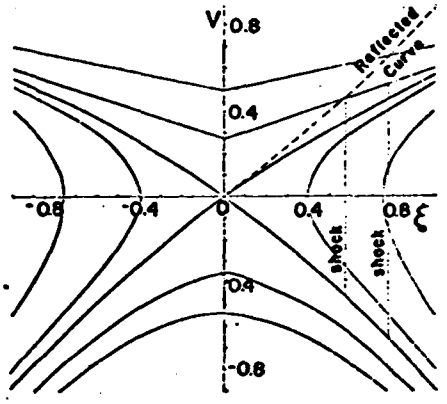

Figure 6. Laval nozzle curves for different end conditions.

IV. Numerical Procedures Investigated

Several techniques were investigated to obtain the solution with shock and the modified least square method was found to give the desired results. A detailed discussion of the other methods investigated is beyond the scope of this paper, but a brief mention is made with reference to them here.

The fourier sine transform technique was used to solve the governing equation and it resulted in a solution resembling the subsonic solution. The one and two term least square method using fourier series and imposing the additional conditions that $V = 0$ (M=1) and $dV/d\xi < 0$ at the throat resulted in a solution which did resemble the shock solution but was not a good reproduction of the exact solution. The results are sketched in figure 7. To obtain an acceptable result, a larger number of terms in the fourier series would have to be considered and the effort required to obtain the final form of the non-linear algebraic equations would be prohibitive. Hence the simpler least square finite element technique was preferred over the other methods.

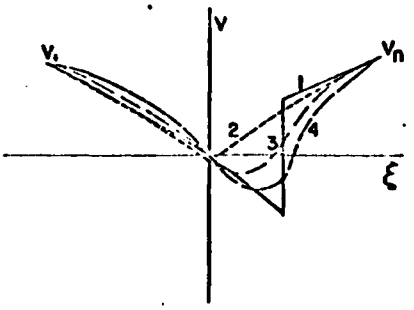

1. Analytical Solution with Shock.
2. Fourier Sine Transform Method.
3. 2-Term Least Square method.
4. 1-Term Least Square Method

Figure 7. Plot of V versus ξ for two other numerical techniques investigated.

V. The Least Square Finite Element Technique

The model equation considered was

$$\frac{d(v^2)}{d\xi} - \xi(1-V) = 0 \qquad (14)$$

with the boundary conditions $V(-a) = V_1$ and $V(a) = V_n$. The range between $\xi = -a$ to $\xi = a$ was divided into a finite number of intervals and for illustration purposes figure 8 shows 4 elements under consideration. V_1 and V_5 are the specified entry and exit conditions respectively and V_2, V_3 and V_4 were computed as follows.

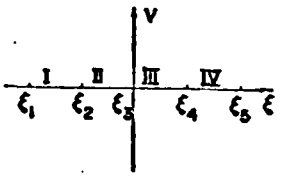

Figure 8. The ξ axis divided into 4 intervals.

Taking two elements simultaneously (figure 9) and assuming a linear variation of V, the system of non-linear algebraic equations was obtained

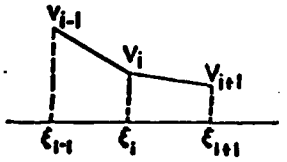

Figure 9. Development of the system of equations.

$$V = a + b\xi \qquad (20)$$

where a and b are functions of V and ξ, that is in the interval ξ_{i-1} to ξ_i

$$a = \frac{V_i\xi_{i-1} - V_{i-1}\xi_i}{\xi_{i-1} - \xi_i}, \quad b = \frac{V_i - V_{i-1}}{\xi_i - \xi_{i-1}} \qquad (21)$$

and similarly in the interval ξ_i to ξ_{i+1}

$$a = \frac{V_i\xi_{i+1} - V_{i+1}\xi_i}{\xi_{i+1} - \xi_i}, \quad b = \frac{V_i - V_{i+1}}{\xi_i - \xi_{i+1}} \qquad (22)$$

Let $$R = \frac{d(v^2)}{d\xi} - \xi(1-V) \qquad (23)$$

where, R is the residue. R = 0 if the solution of the governing equation is exact. Substituting for V from Eq. (20) gives

$$R = 2b(a+b\xi) - (1-a-b\xi)\xi \qquad (24)$$

The total error in the two elements being considered simultaneously is given by

$$\int_{\xi_{i-1}}^{\xi_i} R^2 d\xi + \int_{\xi_i}^{\xi_{i+1}} R^2 d\xi = \text{Total error} \qquad (25)$$

The system of non-linear equations to be solved was obtained by minimizing the total error as

$$\frac{\partial}{\partial V_i}\int_{\xi_{i-1}}^{\xi_i} R^2 d\xi + \frac{\partial}{\partial V_i}\int_{\xi_i}^{\xi_{i+1}} R^2 d\xi = 0 \qquad (26)$$

So, for n unknowns in V, there are n non-linear equations to be solved. Thus for three unknowns the system of equations is

$$F_1(V_2,V_3) = \frac{\partial}{\partial V_2}\int_{\xi_1}^{\xi_2} R^2 d\xi + \frac{\partial}{\partial V_2}\int_{\xi_2}^{\xi_3} R^2 d\xi = 0 \qquad (27)$$

$$F_2(V_2,V_3,V_4) = \frac{\partial}{\partial V_3}\int_{\xi_2}^{\xi_3} R^2 d\xi + \frac{\partial}{\partial V_3}\int_{\xi_3}^{\xi_4} R^2 d\xi = 0 \qquad (28)$$

$$F_3(V_3,V_4) = \frac{\partial}{\partial V_4}\int_{\xi_3}^{\xi_4} R^2 d\xi + \frac{\partial}{\partial V_4}\int_{\xi_4}^{\xi_5} R^2 d\xi = 0 \qquad (29)$$

Newton's method was used to solve the system of algebraic equations and the iterative technique is illustrated below. The $(k+1)^{th}$ iterate is given in terms of the k^{-th} iterate as

$$\{V\}^{(k+1)} = \{V\}^{(k)} - [J]^{-1}\{F\} \qquad (30)$$

where

$$\{V\} = \begin{Bmatrix} V_2 \\ V_3 \\ V_4 \end{Bmatrix}, \quad F = \begin{Bmatrix} F_1 \\ F_2 \\ F_3 \end{Bmatrix}, \quad [J] = \begin{bmatrix} \frac{\partial F_1}{\partial V_2} & \frac{\partial F_1}{\partial V_3} & 0 \\ \frac{\partial F_2}{\partial V_2} & \frac{\partial F_2}{\partial V_3} & \frac{\partial F_2}{\partial V_4} \\ 0 & \frac{\partial F_3}{\partial V_3} & \frac{\partial F_3}{\partial V_4} \end{bmatrix}$$

[J] is a tridiagonal matrix. Let

$$\{V\}^{(k+1)} - \{V\}^{(k)} = \{X\} \qquad (31)$$

Then,

$$[J]\{X\} = -\{F\} \tag{32}$$

$\{X\}$ was obtained from Eq. (32) by Gaussian elimination and $\{V\}^{(k+1)}$ was then obtained from Eq. (31). The initial values of V chosen to start the iterative process were arbitrary. The convergence criterion was

$$\epsilon = \sqrt{\sum_{i=1}^{n}\left(1 - \frac{V_i^{(k)}}{V_i^{(k+1)}}\right)^2} \tag{33}$$

for a system with n unknowns, where $\epsilon \leq 10^{-6}$.

The solution obtained by the conventional least square finite element technique resulted in a solution resembling the subsonic one shown in figure 3. The error in each element was computed by

$$e = \int_{\xi_{i-1}}^{\xi_i} R^2 d\xi \tag{34}$$

for each iteration and it was observed that when starting the iterative process by using the analytically obtained values of the unknowns, the value of e was small in all elements except in the element in which the shock was located, i.e. e was very large in that element (element IV, figure 10). Thus the total error would be very large. The total error

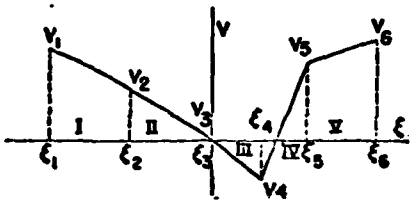

Figure 10. Sketch of a discontinuous solution.

was minimized at each iteration and finally the result converged to a solution resembling the subsonic solution. So a modified least square technique was developed in which the error in the shock element was not considered. The method thus became one of searching and subsequently fitting the shock in the proper element.

VI. The Modified Least Square Finite Element Technique

The same example as in the previous section has been considered to illustrate the method. In the modified least square finite element technique the shock is assumed to lie in a certain element and the error in that element was not considered in the solution of the set of equations.

So, with reference to figure 8, the shock was first assumed to be in element II and neglecting

$$\int_{\xi_2}^{\xi_3} R^2 d\xi ,$$

the system of equations, Eqs. (27),(28) and (29), was solved by Newton's method. Similarly, assuming the shock to be in element III and now neglecting

$$\int_{\xi_3}^{\xi_4} R^2 d\xi ,$$

[illegible] of equations was [illegible] was repeated for all the other [illegible]. Each set of results thus obtained was [illegible] to locate the location of the shock. The next logical step was to check if the jump condition, Eq. (17), was satisfied. For example, considering the shock in element III, the values obtained for V_2, V_3 and V_4 were as shown in figure 11

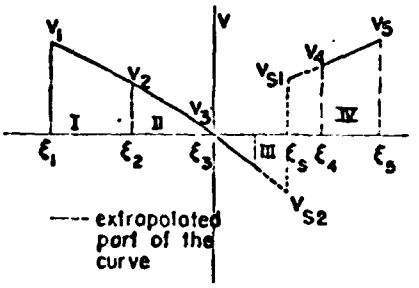

Figure 11: Illustration of the shock fitting approach.

The curve $V_3V_{s_2}$ and $V_4V_{s_1}$ are the extrapolated parts of the solution. If $V_{s_1} = -V_{s_2}$ then it was concluded that a shock would occur in element III, otherwise a shock was not possible in that element. Solution of Eqs. (27), (28) and (29) by the conventional least square method gave one possible result, resembling the subsonic solution, the solution of the same set of equations by the modified least square method using the shock fitting approach gave two possible sets of results with shock, of which the solution with a reverse shock was considered as being physically not acceptable. The two existing possibilities of the flow are shown in figures 12a and 12b, for the example considered.

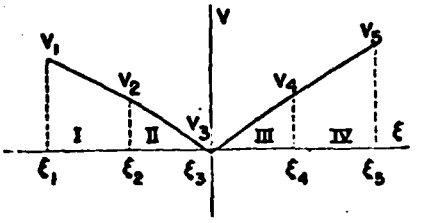

Figure 12a. Subsonic solution.

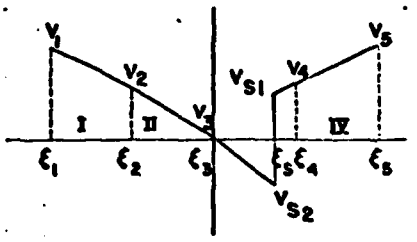

Figure 12b. Shock solution.

To decide on whether to accept the subsonic solution or the shock solution as the appropriate result, the total error was computed for both the cases by

$$E = \sum_{i=1}^{n} \int_{x_1}^{x_{i+1}} R^2 d\xi \qquad (35)$$

which for the example considered becomes

$$E_{\text{no shock}} = E_{Ns} = \int_{\xi_1}^{\xi_2} R^2 d\xi + \int_{\xi_2}^{\xi_3} R^2 d\xi + \int_{\xi_3}^{\xi_4} R^2 d\xi + \int_{\xi_4}^{\xi_5} R^2 d\xi \qquad (36)$$

$$E_{\text{shock}} = E_s = \int_{\xi_1}^{\xi_2} R^2 d\xi + \int_{\xi_2}^{\xi_3} R^2 d\xi + \int_{\xi_3}^{\xi_s} R^2 d\xi + \int_{\xi_s}^{\xi_4} R^2 d\xi + \int_{\xi_4}^{\xi_5} R^2 d\xi \qquad (37)$$

Of the two possible results, the solution with the least total error was selected, that is if $E_{Ns} < E_s$, then a subsonic solution was the correct result and if $E_{Ns} > E_s$, then a shock solution was the correct one.

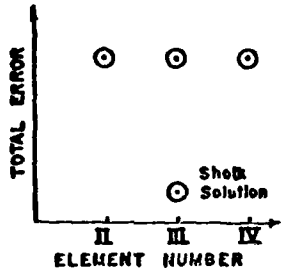

Figure 13. Plot of total error versus element number.

VII. Results for the One-Dimensional Problem

The governing equation (14) was solved numerically by the technique developed for the set of end conditions:

$$V(-1.0) = 0.55122\ , \quad V(1.0) = 0.6 \qquad (38)$$

$$V(-0.0737) = 0.051222\ , \quad V(0.0737) = 0.0513 \qquad (39)$$

Both the possibilities, the subsonic solution and solution with shock, were investigated and the proper solution was selected basing the deduction on the total error in each case. Figures 14 and 15 are the plots of V versus ξ for the different boundary conditions. For the boundary condition in Eq. (39), the values of the Mach number, M, versus X were plotted for $\alpha = 0.25$, indicated in figures 16 and 17.

$$\frac{d(v^2)}{d\xi} - \xi(1-v) = 0$$

$V(1.0) = 0.6 \qquad V(-1.0) = 0.55122$

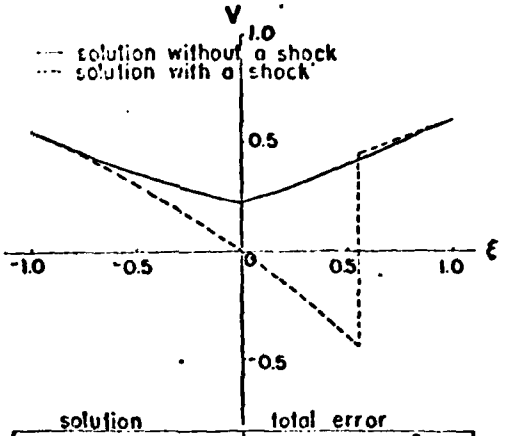

solution	total error
without shock	0.434×10^{-2}
with shock	0.343×10^{-2}

Figure 14. Plot of V versus ξ

$V(-0.0737) = 0.051222$

$V(0.0737) = 0.0513$

$$\frac{d(v^2)}{d\xi} - \xi(1-v) = 0$$

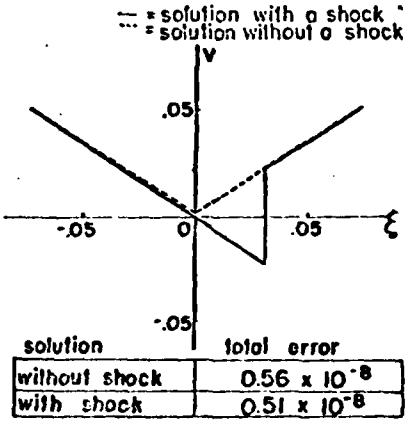

solution	total error
without shock	0.56×10^{-8}
with shock	0.51×10^{-8}

Figure 15. Plot of V versus ξ.

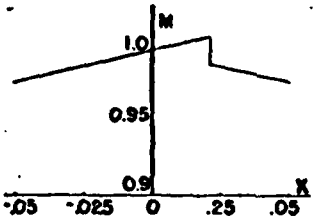

Figure 16. Distribution of the Mach number along the axis of a one dimensional laval nozzle, $\alpha = 0.1$.

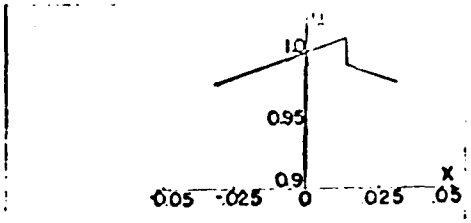

Figure 17. Distribution of the Mach number along the axis of a one dimensional laval nozzle, $\alpha = 0.25$.

VIII. A Note on the Results of the One Dimensional Analysis

The results obtained in the previous section show that the numerical technique developed can successfully be used for similar problems with shocks. The analysis of many flow problems assuming the flow to be one dimensional, is a useful approximation. At first sight this is surprising, since the flow model which forms the basis of the one dimensional method, differs profoundly from the actual physical situation. For example, the one dimensional method, ignores the existence of a non-uniform and possibly changing velocity profile and it assumes happenings at the walls of the channel, e.g. friction, to be felt instantaneously over the whole cross-section. However, the one dimensional method was preferred for its simplicity. The numerically obtained results and the analytical results shown in figure 6, are in excellent agreement. The following sections are devoted to the derivation and solution of the two dimensional laval nozzle problem.

IX. Derivation of the Potential Equation

The nozzle axis was selected as the x-axis and the origin of the coordinate system was placed in the center of the throat. With the hypothesis of non vortical flow and pefect flow of a perfect gas with constant specific heats C_p, C_v and $\gamma = C_p/C_v$, the potential equation for two dimensional flow is

$$\frac{\partial \tilde{u}}{\partial x}(a^2-\tilde{u}^2) + \frac{\partial \tilde{v}}{\partial y}(a^2-\tilde{v}^2) - 2\tilde{u}\tilde{v}\frac{\partial \tilde{u}}{\partial y} = 0 \qquad (40)$$

In this $\tilde{u}$, $\tilde{v}$ are the x and y components of velocity and a, the local sonic velocity, is related to the critical velocity a_* through

$$a^2 = \frac{\gamma+1}{2}a_*^2 - \frac{\gamma-1}{2}(\tilde{u}^2+\tilde{v}^2) \qquad (41)$$

Substituting Eq. (41) in Eq. (40), limiting the present investigation to the vicinity of the throat and introducing the dimensionless velocity components

$$\tilde{u} = a_*(1+u) \text{ and } \tilde{v} = a_* v \qquad (42)$$

in which u and v are small quantities, the potential equation; Eq. (40), becomes

$$\frac{\partial u}{\partial x}\left(2u + u^2 + \frac{\gamma-1}{\gamma+1}v^2\right) - \frac{\partial v}{\partial y}\left[\frac{2}{\gamma+1} - \frac{2(\gamma-1)}{\gamma+1}u - \frac{\gamma-1}{\gamma+1}u^2 - v^2\right) + \frac{4}{\gamma+1}\frac{\partial u}{\partial y}(1+u)v = 0 \qquad (43)$$

As $x \to 0$, $y \to 0$; u [illegible] zero and also on the basis of Eq. (43) [illegible] consequently the quotient v/y approach[illegible], while the velocity rise $\partial u/\partial x$ along the axis [illegible] not to vanish at the origin. Then, if the small quantities u and v are considered linear only, the following approximate relation is obtained from Eq. (43).

$$(\gamma+1)u\frac{\partial u}{\partial x} - \frac{\partial v}{\partial y} + 2v\frac{\partial u}{\partial y} = 0 \qquad (44)$$

Since the nozzle flow is symmetrical with respect to the x-axis, $\partial u/\partial y$ also approaches zero as $x \to 0$, $y \to 0$. Consequently the term $2v\,\partial u/\partial y$ may be ignored by means of which Eq. (44) becomes

$$\frac{\partial v}{\partial y} - \frac{\gamma+1}{2}\frac{\partial (u^2)}{\partial x} = 0 \qquad (45)$$

Similarly the condition of irrotationality becomes

$$\frac{\partial v}{\partial x} - \frac{\partial u}{\partial y} = 0 \qquad (46)$$

At the walls, in the vicinity of the throat for small u and v it can be shown that

$$y' = v \qquad (47)$$

where $(\,)'$ denotes differentiation with respect to x.

X. Application of the Method of Integral Relations

The method of integral relations was originated by Dorodnitsyn in 1958 and was subsequently applied to several fluid dynamics problems. Several scientists including Holt, Liddle and Archer have applied the MIR to the nozzle problem. This method provides a powerful tool for solving problems governed by nonlinear partial differential equations with the aid of computers and appears to be well suited to the laval nozzle problem. It is applicable to problems of elliptic or mixed elliptic-hyperbolic type in two independent variables. Certain dependent variables are represented as polynomials or fourier series in one of the independent variables and the original system of partial differential equations is replaced by a system of ordinary differential equations for the coefficients. These ordinary differential equations are then solved using the appropriate boundary conditions.

For the one strip case the notations used are shown in figure 18.

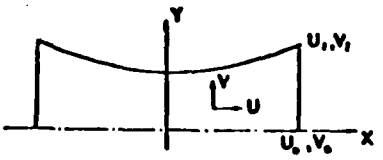

Figure 18. One strip notations.

x,y to x,η where

$$\eta = y/Y \tag{48}$$

Then, as η = 0 on the x-axis and η = 1 on the channel wall Eqs. (45), (46) and (47) become

$$\frac{2}{Y}\frac{\partial v}{\partial \eta} - (\gamma+1)\frac{\partial(u^2)}{\partial x} + \frac{Y'}{Y}(\gamma+1)\eta\frac{\partial(u^2)}{\partial \eta} = 0 \tag{49}$$

$$\frac{\partial v}{\partial x} - \frac{Y'}{Y}\eta\frac{\partial v}{\partial \eta} - \frac{1}{Y}\frac{\partial u}{\partial \eta} = 0 \tag{50}$$

$$v_1 = Y' \tag{51}$$

Integrating Eqs. (49) and (50) with respect to η between zero and a general value at a constant x-station gives

$$\int_0^\eta \frac{2}{Y}\frac{\partial v}{\partial \eta}\,d\eta - \int_0^\eta (\gamma+1)\frac{\partial(u^2)}{\partial x}\,d\eta + \int_0^\eta \frac{Y'}{Y}(\gamma+1)\eta\frac{\partial(u^2)}{\partial \eta}\,d\eta = 0 \tag{52}$$

$$\int_0^\eta \frac{\partial v}{\partial x}\,d\eta - \int_0^\eta \frac{Y'}{Y}\eta\frac{\partial v}{\partial \eta}\,d\eta - \int_0^\eta \frac{1}{Y}\frac{\partial u}{\partial \eta}\,d\eta = 0 \tag{53}$$

For the one strip case a linear approximation for u and v was assumed. For the two strip case a quadratic interpolation could be done. Denoting the values on the axis by suffix 0 and the values on the channel wall by suffix 1,

$$u = u_0 + \eta(u_1 - u_0) \tag{54}$$

$$v = v_0 + \eta(v_1 - v_0) \tag{55}$$

But $v_0 = 0$ by symmetry. Substituting Eq. (51) in Eq. (55) gives

$$v = \eta Y' \tag{56}$$

Substituting for u and v and placing η = 1 in Eqs. (52) and (53) gives

$$\frac{\gamma+1}{3}[u_o'(2u_o+u_1) + u_1'(u_o+2u_1)] + \frac{\gamma+1}{3}\frac{Y'}{Y}[u_o^2 + u_o u_1 - 2u_1^2] - \frac{2Y'}{Y} = 0 \tag{57}$$

$$u_1 = u_o + \frac{1}{2}[YY'' - (Y')^2] \tag{58}$$

Assuming a parabolic channel wall

$$Y = 1 + \alpha x^2 \tag{59}$$

where α is a constant depending on nozzle geometry, (57) and (58) were solved for unknowns u_o and u_1. The two possibilities considered while reducing these equations further were $\alpha x^2 << 1$ and when order x^2 terms were not negligible.

The one strip equations (57) [illegible] for a parabolic wall shaped nozzle reduce to

$$u_1 = u_o + \alpha(1-\alpha x^2) \tag{60}$$

$$\frac{d(V^2)}{d\xi} - \xi(1-V) = 0 \tag{61}$$

where,

$$V = -\frac{2u_o + \alpha(1-\alpha x^2)}{\frac{\alpha(1-\alpha x^2)}{3} + \frac{2}{\alpha(\gamma+1)}} \tag{62}$$

$$\xi^2 = F\,\ell n\left|\frac{2cx^2+E}{2cx^2+G}\right| - F\,\ell n\left|\frac{E}{G}\right| \tag{63}$$

$$F = \frac{48\alpha^3(\gamma+1)}{2\sqrt{-q}},\quad E = 6\alpha - \sqrt{-q} \tag{64}$$

$$G = 6\alpha + \sqrt{-q},\quad c = -(\gamma+1)\alpha^4 \tag{65}$$

$$q = 4c[6 + \alpha^2(\gamma+1)] - 36\alpha^2 \tag{66}$$

with the jump condition for weak solutions given by

$$[V^2] = 0 \tag{67}$$

As indicated by the above analysis, it was possible to reduce the one-strip equations to a form similar to the one dimensional governing equation and this was subsequently solved by the least square finite element technique.

Corresponding to the solution of Eq. (61) with the boundary conditions (39) as shown in figure 15, the curves for u_o and u_1 are plotted for α = 0.1 and α = 0.25 in figures 19 and 20.

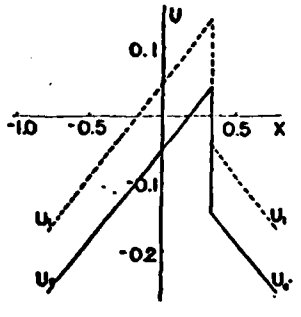

Figure 19. Distribution of u along the x-axis and the channel wall of a symmetric two dimensional laval nozzle with parabolic arc wall, α = 0.1.

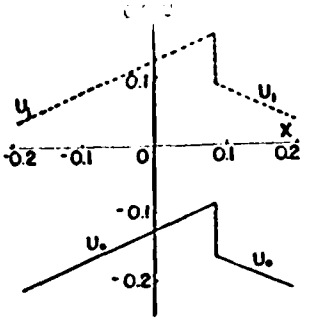

Figure 20. Distribution of u along the x-axis and the channel wall of a symmetric two dimensional laval nozzle with parabolic arc walls, $\alpha = 0.25$.

XII. The One Strip Case Assuming $\alpha x^2 << 1$

Assuming $\alpha x^2 << 1$, the one strip equations for a parabolic wall shaped nozzle reduce to

$$u_1 = u_o + \alpha \tag{68}$$

$$\frac{d(V^2)}{d\xi} - \xi(1-V) = 0 \tag{69}$$

where

$$V = -\frac{(u_o + \frac{\alpha}{2})}{(\frac{1}{\alpha(\gamma+1)} + \frac{\alpha}{6})} \tag{70}$$

$$\xi = \sqrt{\frac{4\alpha^2}{\frac{1}{\alpha(\gamma+1)} + \frac{\alpha}{6}}}\ X \tag{71}$$

with the jump condition for weak solutions given by

$$[V^2] = 0 \tag{72}$$

The relation between M and M_* is

$$M^2 = \frac{2}{\frac{\gamma+1}{M_*^2} - (\gamma-1)} \tag{73}$$

and it can be easily shown that

$$u_1 = M_{*1} - 1 \tag{74}$$

$$u_o = M_{*o} - 1 \tag{75}$$

The least square technique was used to solve the governing differential equation, Eq. (69).

Corresponding to the solution of Eq. (69) with the same boundary conditions as in (39), the curves for u_o and u_1 are plotted for $\alpha = 0.1$ and $\alpha = 0.25$ in figures 21 and 23 and the corresponding curves for M_o and M_1 are plotted in figures 22 and 24.

An average value of the x-velocity was computed with

$$u_{average} = u_o + \frac{\alpha}{2} \tag{76}$$

and the average velocity and Mach ... been plotted in the corresponding figures ... sults clearly show that the jumps in velocity ... at the same value of x for the one strip ...

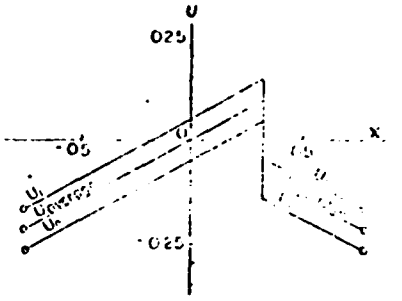

Figure 21. Distribution of u along the x-axis and the channel wall of a symmetric two dimensional laval nozzle with parabolic-arc walls, $\alpha = 0.1$.

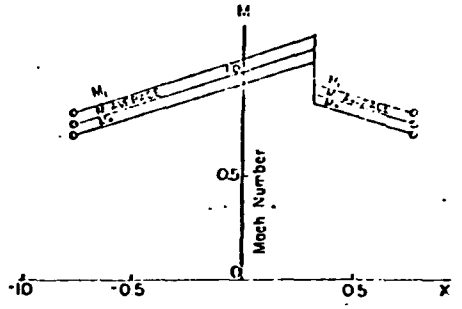

Figure 22. Distribution of the Mach number along the x-axis and the channel wall of a symmetric two dimensional laval nozzle with parabolic-arc walls, $\alpha = 0.1$.

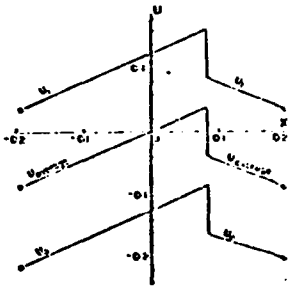

Figure 23. Distribution of u along the x-axis and the channel wall of a symmetric two dimensional laval nozzle with parabolic-arc walls, $\alpha = 0.25$.

For $\alpha = 0.1$ and 0.25 the results indicated in figures 21 and 23 show good agreement with the results of figures 19 and 20 in the preceding section. Thus it can be safely concluded that $\alpha x^2 << 1$ is a good approximation and it is not necessary to go through a more complicated and tedious analysis of the previous section to get good results. The average values of the velocity plotted in figures 21 and

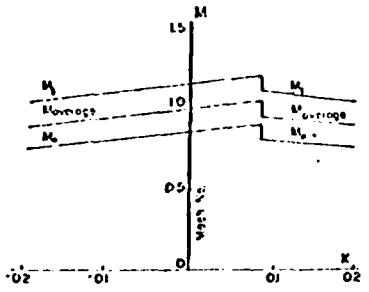

Figure 24. Distribution of the Mach number along the x-axis and the channel wall of a symmetric two dimensional laval nozzle with parabolic-arc walls, $\alpha = 0.25$.

23 are interpreted as the average velocity of the flow in the channel. Furthermore the shock occuring at some average value between the wall and the axis is a normal shock and the shock is located at the point where there is a jump in the average velocity, $(u_o + \alpha/2)$. Figure 25 illustrates the importance of the average velocity

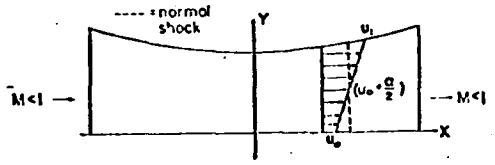

Figure 25. The normal shock and the linear velocity distribution in a symmetric two dimensional laval nozzle.

The first study of the continuously-accelerating flow in a laval nozzle was made by Meyer[18]. The least square finite element method can also be used to obtain the solution of such problems. The numerical and the analytical results are compared in Appendix A.

XIII. Application of the Least Square Finite Element Method to Emmons' Hyperbolic Channel Flow

The method of integral relations is now applied to a channel flow first calculated by Emmons[14]. The symmetric hyperbolic channel can be described by

$$Y = a\sqrt{1 + \frac{x^2}{b^2}} \tag{77}$$

where, $a = 0.5646425$ and $b = 0.8253356$

The one strip equations, Eqs. (57) and (58), for the Emmons hyperbolic nozzle in the vicinity of the throat reduce to

$$u_1 = u_o + \frac{a^2}{2b^2} \tag{78}$$

$$\frac{d(V^2)}{d\xi} - \xi(1-V) = 0 \tag{79}$$

where,

$$V = \frac{\left[u_o + \frac{a^2}{4b^2}\right]}{\frac{1}{6}\left[\frac{8b^2}{a^2(\gamma+1)} + \frac{a^2}{2b^2}\right]} \tag{80}$$

and

$$\xi = \frac{3a}{b^2}\sqrt{\frac{1}{\left(\frac{8b^2}{a^2(\gamma+1)} + \frac{a^2}{2b^2}\right)}}\; x \tag{81}$$

Eq. (79) was solved by the least square technique developed.

Corresponding to the solution of Eq. (79) with the boundary conditions $V(-0.3660) = 0.23745$, $V(0.3660) = 0.24250$, the curves for u_o, u_1 and $u_{average}$ and M_o, M_1 and $M_{average}$ are plotted in figures 26 and 27, where

$$u_{average} = u_o + \frac{a^2}{4b^2} \tag{82}$$

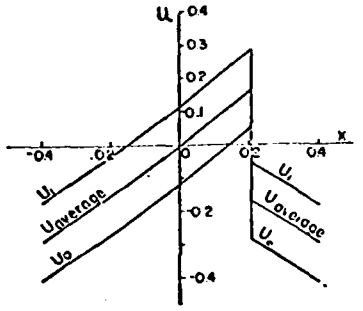

Figure 26. Distribution of u along the x-axis and the channel wall of a symmetric two dimensional laval nozzle with hyperbolic-arc walls.

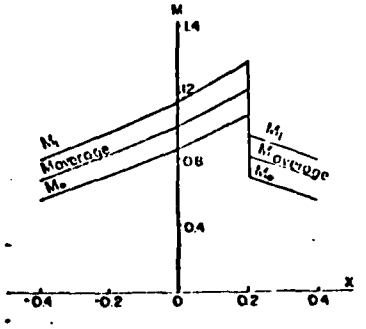

Figure 27. Distribution of the Mach number along the x-axis and the channel wall of a symmetric two dimensional laval nozzle with hyperbolic-arc walls.

Emmons[14] had solved the problem of a two dimensional flow of a frictionless, adiabatic, perfect gas inside a hyperbolic nozzle. Emmons' solution was for curved shocks and since the velocity field after such shocks is not in general irrotational, he had considered the rotation term in the flow following the shock wave. The numerical solution

of Emmons' upstream [illegible] the least square finite element solution for the one strip case show an excellent agreement. Emmons' solution is shown in figure 28

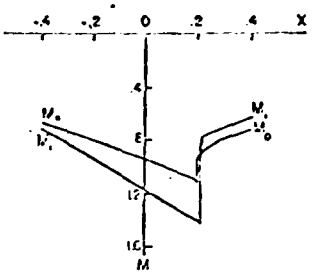

Figure 28. Flow of a compressible fluid in a hyperbolic channel as obtained by Emmons.

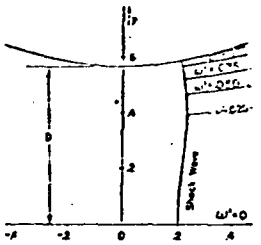

Figure 29. Distribution of rotation; constant rotation lines; ω = rotation $\omega' = \omega D/a_o$, dimensionless rotation, (a_o = stagnation acoustic velocity).

The flow downstream of the shock wave was not in agreement with Emmons' solution due to the following reasons. While Emmons considered the complete differential equation of compressible flow to obtain his results, the least square method was used to solve the approximate differential equation which gives excellent results for transonic flows in the vicinity of the throat of a laval nozzle. As already indicated before, only weak solutions were investigated in this paper, while the results obtained by Emmons was for strong shocks. Secondly, while Emmons had considered rotational flow downstream of the shock (figure 29), this paper assumed the flow to be irrotational before and after the shock.

XIV. Conclusions

A least square finite element technique was developed to solve problems of transonic flow with shocks. On an average it took less than five seconds of CPU time on the IBM 370/Systems 167 computer to obtain the result for a problem with nine elements using this method. The solutions obtained for the two illustrative examples show that this method is a powerful and inexpensive tool to solve similar problems with shocks. The equations have to be reduced in such a manner that the jump conditions can be extracted from them and at times this involves juggling with algebraic quantities, although once this is done the solution is quite simple. The method can be extended to the two strip case and can also be applied to the unsteady flow problem.

Acknowledgements

Acknowledgements are due to Professor S.F.Shen, the author's committee chairman and thesis advisor, Professor Charles Vanloan, the author's minor committee member and to Professor David Caughey for their help and advice during the course of this research.

Appendix A

If the nondimensional velocity perturbations u and v are defined by

$$u = \frac{\tilde{u}}{a_*} - 1, \quad v = \frac{\tilde{v}}{a_*} \tag{83}$$

In terms of these conditions the irrotationality is

$$\frac{\partial u}{\partial y} = \frac{\partial v}{\partial x} \tag{84}$$

which enables a potential ϕ to be defined by

$$u = \frac{\partial \phi}{\partial x}, \quad v = \frac{\partial \phi}{\partial y}.$$

The equation of continuity is

$$(-2\phi_x - \phi_x^2 - \frac{\gamma-1}{\gamma+1}\phi_y^2)\phi_{xx} - \frac{4}{\gamma+1}(1+\phi_x)\phi_y\phi_{xy} + (\frac{2}{\gamma+1} - \frac{2(\gamma-1)}{\gamma+1}\phi_x - \frac{\gamma-1}{\gamma+1}\phi_x^2 - \phi_y^2)\phi_{yy} = 0 \tag{85}$$

Meyer[18] in his investigation of the continuously-accelerating flow in a laval nozzle assumed that the velocity distribution along the axis increased linearly, i.e.

$$u = Kx, \quad \phi = \frac{1}{2}Kx^2 \tag{86}$$

and by direct substitution in Eq. (85) of a double power series for ϕ.

$$\phi = \Sigma\Sigma\, \phi_{mn} x^m y^n, \tag{87}$$

he obtained the coefficients ϕ_{mn} up to and including the sixth order terms ($m+n \leq 6$).

$$\phi = \frac{1}{2}Kx^2 + \frac{\gamma+1}{2}K^2xy^2 + \frac{(\gamma+1)^2}{24}K^3y^4 + \frac{(\gamma+1)(2\gamma-1)}{4}K^3x^2y^2 + \cdots \tag{88}$$

It was shown later that the exact solution of the approximate differential Eq. (89)

$$-2\phi_x\phi_{xx} + \frac{2}{\gamma+1}\phi_{yy} = 0 \tag{89}$$

is the first three terms of the one given in Eq.(88).

[illegible] Eq. (89) [illegible] Eq. (87) in terms of the velocity perturbations u and v. Thus the exact solution for the two dimensional transonic flow problem for a continuously-accelerating flow becomes

$$u = Kx + \frac{\gamma+1}{2} K^2 y^2 \qquad (90)$$

$$v = (\gamma+1)K^2 xy + \frac{(\gamma+1)^2}{6} K^2 y^3 \qquad (91)$$

The equation of the line along which the flow is parallel to the x-axis is given by

$$x = -\frac{\gamma+1}{6} Ky^2 \qquad (92)$$

It was also shown that the length parameter K^{-1} is related to the radius of curvature R_1 of the streamlines in the throat region by

$$K = \frac{1}{\sqrt{(\gamma+1)R_1}} \qquad (93)$$

where R_1 is the radius of curvature of the wall profile at the throat made nondimensional by dividing by the nozzle half height or the radius at the throat as the case may be.

With $R_1 = 5$, the velocity distribution along the x-axis and the channel walls of a symmetric two dimensional nozzle with parabolic-arc walls has been plotted in figure 30.

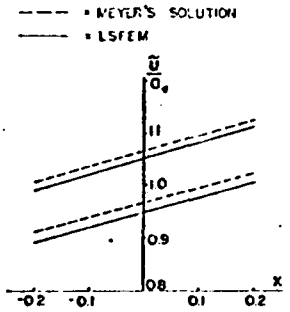

Figure 30. Velocity distributions along the x-axis and the channel walls of a symmetric two dimensional nozzle with parabolic-arc walls, $R_1 = 5$.

Equation (90) shows that u varies quadratically in y while in the one strip case it was assumed that u varies linearly in y. Thus Meyer's results and the results obtained numerically by the least square finite element method (LSFEM) do not show perfect agreement. In the two strip case where u and v can be considered to vary quadratically in y, while in the Meyer's solution and the LSFEM solution are expected to be in close agreement with each other.

1. [illegible], E.M. and Sutton, E.P., "Transonic [illegible] and Nozzles: A Survey", Transactions of Symposium Transsonicum, Aachen, Sept. [illegible], edited by K. Oswatitsch, Springer-Verlag, [illegible], pp. 325-44.
2. Sichel, M., "Theory of Viscous Transonic [illegible] - A Survey", AGARD Conference Proceedings, No. 35, Transonic Aerodynamics, Paper 10, 1968.
3. Midgal, D., Klein, K., and Moretti, S., "Time-Dependent Calculations for Transonic Nozzle Flow", AIAA Journal, Vol. 7, No. 2, Feb. 1969, pp. 372-4.
4. Midgal, D. and Kossen, R., "Shock Predictions in Conical Nozzles", AIAA Journal, Vol. 3, No. 8, Aug. 1965, pp. 1554-1556.
5. Thompson, P.A., "Transonic Flow in Curved Channels", Transaction of the ASME: Journal of Basic Engineering, Paper 67-FE-11, Vol. 89, Dec. 1967, pp. 748-752.
6. Holt, M., "The Design of Plane and Axisymmetric Nozzles by the Method of Integral Relations", Transactions of Symposium Transsonicum, Aachen, Sept. 1962, edited by K. Oswatitsch, Springer-Verlag, 1964, also Rept. AFOSR 3140, Sept. 1962, Univ. of California, Institute of Engineering Research, Berkeley, California.
7. Lighthill, M.J., Proc. Roy. Soc. A 191, 323, 1947.
8. Frankl, F., Dokl. Akad. Nauk., USSR 9, 387, 1945.
9. Cherry, T.M., Phil. Trans. Roy. Soc. London A 904, 1953.
10. Cherry, T.M., J. Australian Math. Soc. 1, 80, 1959.
11. Cherry, T.M., J. Australian Math. Soc. 1, 357, 1960.
12. Taylor, G.I., British Aeronautical Research Committee R and M, 1381, 1930.
13. Oswatitsch, K. and Rothstein, W., "Flow Pattern in a Converging-Diverging Nozzle", TM 1215, 1949, NACA.
14. Emmons, H.W., "The Theoretical Flow of a Frictionless, Adiabatic, Perfect Gas Inside of a Two-Dimensional Hyperbolic Nozzle", NACA-Technical Note No. 1003, May 1946.
15. Liddle, S.G. and Archer, R.D., "Transonic Flow in Nozzles Using the Method of Integral Relations", Journal of Spacecraft and Rockets, Vol. 8, No. 7, pp. 722-728, July 1971.
16. Liddle, S.G., "Integral Relations Method Computations of Annular and Asymmetric Plane Nozzle Flowfields", Journal of Spacecraft and Rockets, Vol. 11, No. 3, pp. 146-151, 1973.
17. Chen, H.C., "Finite Elements for Compressible Flow", Ph.D. Thesis, Cornell University, Ithaca, N.Y., 1975.
18. Meyer, Th., V.D.I. Forschungsheft 62, 1908.